An Iterative Approach to Scattering by Edges and Wedges

J. Dylan Morgan and Anthony D. Rawlins

Mathematics Department, Brunel University, Uxbridge, UB8 3PH, UK.

Abstract

A new approach to the calculation of the scattering of waves by the edge of a thin plate or the edge of a wedge of any angle is presented. It has a number of advantages relative to previous methods. It is intuitively easy to grasp, being close in spirit to ray optics methods for solving problems. It deals with the whole range of configurations in the one way, rather than the patchwork of ways that has evolved in the past. It provides extremely good approximate solutions with minimal effort. The mathematics involved is reasonably simple. It promises to be applicable to a range of problems which have yet to be solved by other methods. In particular we show how it can be applied in principle to obtain successive approximations to the solution of the problem of diffraction by a permeable wedge, where its relationship to the ray optics method is very clear.

1 Introduction

In this paper we will be dealing primarily with the theory of the scattering of waves from sharp straight-line edges. As is usual in theoretical treatments of such problems the edge is modelled by an infinite straight line, though the results can be applied, with appropriate reservations, to the finite edges of the physical world. The theory can be applied, with suitable small appropriate modifications, to waves which are electromagnetic, acoustic, seismic and so on. Typical examples of edges are thin plates and wedges. The waves may or may not be supposed to penetrate the wedges.

The force of this paper is to present an approach to this wide class of problems which has many virtues. It is simpler than most existing approaches. It can deal with the whole range of such problems in one single coherent way, rather

[1] Supported by the Engineering and Physical Sciences Research Council

than in a number of different ways. It can provide approximate results in a yet simpler way, which are often likely to be of great use to experimenters. It is analytically precise. It is intuitively appealing. It shows promise of being applicable to hitherto unsolved problems.

The history of research in this area over the last hundred years or so reveals a step-like progress. A new technique is discovered, and presented in a single paper, which deals with a particular problem. This technique is then applied, by a number of people in a large number of papers, to a number of related problems in a fairly routine way. Some time later a new technique is discovered which can be applied to another range of such scattering problems and this is again applied for some years to related problems in a variety of different contexts. One example is the use of the separation of variables Macdonald[1] or the Kontorowich-Lebedev technique [2] involving Bessel Functions to solve the problem of scattering by a two-dimensional infinite wedge into which the wave does not penetrate. Another example of a particular approach is the Wiener-Hopf technique [3] which was evolved to solve the problem of scattering by an infinitely thin two-dimensional semi-infinite plate, which is a mathematical approximation to a physically real thin plate with finite thickness and length.

It will be noticed that the problem solved mathematically is always and inevitably an idealization and an approximation to any real physical problem. Every physical wedge, for example a glass prism, is always finite. But to provide an exact mathematical solution to such a problem can be regarded as virtually impossible. So what has been done is to isolate the key feature - the sharp edge - and to do the calculations for an idealization of this feature. This idealization is a good one when the length of a face is large compared with a wavelength of the incident field. And the results can be used to give a good idea of the magnitudes found in practice, if used with due caution. However, it must be emphasized that although there is an intellectual satisfaction in obtaining a perfectly accurate solution to the idealized problem, it must be remembered that the ultimate justification of the work is to obtain numbers that can be applied in a practical or experimental setting.

The second point to make is that the solutions that are derived by the increasingly sophisticated mathematical techniques have become more and more complex in form. Let us look at what is meant by a solution. If we are talking about the scattering of an incident wave of light by a perfect infinite mirror then the solution can be written down by simply considering the field of an image source. We thus need only simple algebra. When we come to consider the scattering of light by a semi-infinite mirrored surface (using the Wiener-Hopf technique) then the solution is an infinite integral using a kernel that can be calculated using only simple algebra. It is still possible to approximate this solution, especially in the far field, so that the integral is replaced by an algebraic expression. Before the advent of computers this was done routinely.

Today we may perhaps regard a solution in terms of an integral as almost as good.

But, as more difficult problems have been tackled, the the solutions have become increasingly complicated in structure. Thus if we try to solve the problem of scattering by a semi-infinite plane with mixed boundary conditions (Rawlins[4]) we find that the solution is an integral over a kernel which itself can only be evaluated by performing another integration. Likewise if we try to solve the problem of scattering of light by a dielectric wedge then existing techniques (Rawlins[5]) can not even find the solution in that way. The best they can do is to reduce the problem to that of solving coupled integral equations in order to find a complicated kernel which will then have to be integrated numerically to find the full solution.

In short, the computational difficulty is steadily increasing until such approaches come into conflict with *ab initio* numerical methods, in which sheer computational power is thrown at solving the wave equation directly. Proponents of that approach can argue that they can do far more than the theoretical approaches mentioned above when it comes to dealing with real finite obstacles, as they do not need to make the simplifications of infinitely thin surfaces, infinite faces and so on.

Of course the traditional counter-argument is that the exact solutions provide more insight. They give an *understanding* of the patterns involved which are ultimately of more value than particular numerical calculations. However, the increasingly complicated nature of the approaches that have been found necessary in order to find exact solutions are resulting in less and less physical insight. So we are losing insight and gaining in computational difficulty as time has passed. The theoretical approaches have therefore tended to give less and less value in the real world where, in the end, they are designed to be of worth.

It can help to clarify the goal of this paper to focus on the practical requirements of experimenters and designers of equipment and shielding in a world where what is required is a good prediction of amplitudes and *not* a perfectly accurate solution to a problem which is in any case only an approximation to any practical real-world situation. It is natural to start with the ray optics approximation to the kind of problems that we are dealing with. It is easy to draw the rays. It it easy to see where shadow boundaries lie. It is easy to calculate the amplitude of plane waves outside the shadow regions. In all of the fields of interest - acoustics, electromagnetic, etc - this simple approximation tells the experimenter or designer a great deal about what he can expect to find in practice and gives him order of magnitude estimates of amplitudes as well. It is natural then to require of a theory that it be able to give a somewhat better approximation. The first obvious question is, How does the field behave near shadow boundaries? This is a simple question but when we turn to the literature we at once find ourselves immersed in some surprisingly complicated mathematics before we can get the required answer, and the clarity of the initial ray optics approximation has gone for good.

This preamble provides the motivation for the remainder of this paper. We propose an approach to this class of problems, which we believe to be fresh one and turns out to have the following properties:

- First and foremost, it will be able to answer the natural question of the physicist or engineer, "How do we accurately correct for the shadow boundaries cast by edges or wedges in a ray optics approximation to scattering by edge or wedges?"
- It will deal with all problems of scattering from edges or wedges in the same way, rather than needing different techniques for different configurations.
- Solutions will involve no more complex mathematical operations than simple algebra and one level of integration.
- It will therefore be reasonably easy to obtain numerical results with a computer.

It may seem, *a priori*, surprising that our approach has not been followed before, but to the best of our knowledge it has not. The reason, we suppose, is that the first step is largely counter-intuitive. (However it must be noted with hindsight that it might be regarded as an extension of some work done over a century ago by one of the earliest workers in our field. Somerfeld[9] solved a problem of scattering from a semi-infinite plate starting with a certain non-physical space. We, also, start with a non-physical space, albeit a different one.)

The first step is the solving of a non-physical problem. That is the problem of scattering of a wave in a space which has a line singularity. Such a space is not physical. However we are used to thinking of such spaces in the context of complex function theory, where a branch point gives rise to a multi-sheeted space, and familiarity with that idea can be helpful here. So we consider the wave equation in cylindrical polar coordinates relative to a line singularity. The key point is that whereas we would in physical space insist that the solution be single valued, which is to say it will be a periodic function of the angular variable, in this Polar Space we drop that restriction. Why should we do this? The spirit is that of all exact mathematical models. We extract the key or central feature. And in all the edge and wedge problems the common feature is a line which is in some sense singular. The idealized model we start with can then be thought of as nothing more or less than the problem of scattering by such a line.

We show that this problem can be readily solved in terms of a simple integral.

The integral is a form of the Sommerfeld integral, which is often found in studies of the wave equation in cylindrical polar coordinates and has been used to solve many problems, but, to the best of our knowledge, *not this simple non-physical one.* We will show how the solutions thus obtained model the behavior of the scattered wave in the shadow regions behind the line in Polar Space, and thus see already how we have a simple tool with which to model shadow boundaries in more complex problems.

The next step is then to use this simple solution to generate the solutions to scattering problems in physical space by iteration. It is this iterative approach that seems to us to be central to the novelty of our method and to its physically intuitive properties. Thus suppose that we are considering the problem of scattering of an incident wave by a semi-infinite plate. The incident wave does not, of course, satisfy the required boundary condition on the bottom surface of the plate. But we can remedy this by adding to the simple solution above an equally simple term which combines with it to satisfy the boundary condition. This gives a first order correction. But of course this correction term will not satisfy the boundary condition on the top of the plate. But we can again use our elementary class of solutions to add a second non-periodic solution to fix the top boundary condition. This second order correction then has to be corrected still further by another term for the bottom condition to be satisfied, and so on. The process then has to be repeated starting with the effect of the incident wave on the top surface. We then have an infinite sequence of integrals which together give the correct and periodic solution.

In the case of simple boundary conditions the series can be simply summed and shown to give the same result as existing methods. This has value in confirming the accuracy of our method. It is also useful as it enables us to compare the exact solution with approximations given by the first few terms of the iterative or series solution. And we find, in fact, that in these cases a few terms give as good a result as would be required for most practical purposes.

Furthermore the approach has a simple intuitive appeal once it becomes familiar. It reminds one, for example, of the way in which the wave equation in the space between two parallel surfaces can be solved by an iterative process of calculating the result of multiple simple reflections, seen as a series of images of the source term, rather than by starting with periodic basis functions which satisfy the boundary conditions. In this approach, similarly, by allowing ourselves the initial freedom to use non-periodic elementary solutions we can build up to a periodic solution by just adding the effect of multiple reflections. To put it another way we are going through a very similar process to that used in solving the problem in a ray optics approximation. The differences are first that we have integrals in place of plane waves and second that we have some terms where the ray optics equivalent would be zero as those terms cannot, by their nature, pass around corners.

By contrast, previous approaches have (not un-naturally) started with looking at single-valued solutions. But such a solution *ipso facto* contains the effect of an infinite number of multiple reflections. It thus loses the great simplicities that can be obtained by considering one reflection at a time.

Those are the simple key ideas behind this paper. The actual steps taken are the following:

- We describe the form of solution to the wave equation in Polar Space that will be used throughout.
- We examine a few special cases that relate to plane waves and line sources.
- We show how this form of solution can be used to satisfy a variety of different boundary conditions on a surface $\theta =$ constant which will be used later. The most difficult case is that of diffraction by the interface between two different media
- We specialize to the case of an incident plane wave and then find the solution to the key problem of scattering by a line singularity.
- We next show in detail how a simple iterative scheme using the above allows us to write down a series solution to the problem of a plane wave incident on a semi-infinite sheet. This series can in fact be summed. An appendix shows how this result is related to the known solution of this problem.
- We compare numerically the full solution with partial solutions obtained from the first term or two of the series expansion and show how remarkably good the latter are in practical terms.
- We then move to the rather general problem of a plane wave incident on an edge *or wedge* with general impedance boundary condition and again show how readily this responds to the iterative approach. The simpler cases can be summed and again can be shown to reproduce existing known solutions. The case of the wedge with impedance boundary conditions has been solved before by Maliuzhinets[11], though the method used is considerably more complicated, involving special functions. Further discussion and references to this problem may be found in Rawlins[12]
- Finally we establish the basis of applying the method to the considerably more complicated problem of scattering by a dielectric wedge. We present the analytic form of the series which formally solves this previously unsolved problem. We exemplify the method by reference to the corrections to the first few ray optics terms.

2 Elementary solutions to scattering problems in Polar Space.

We will be working throughout with harmonic waves with time dependence $e^{-i\omega t}$ with $\omega > 0$. Since any particular wave source can be decomposed into its harmonic components, this involves no loss of generality. If the speed of propagation of the wave in a medium is c, then the field will be a function of $k = \omega/c$. We will generally be supposing that we are making the customary assumption of a two dimensional model and throughout be interested in the wave equation in polar coordinates (r, θ) (which are the natural ones for the class of problems under consideration). The reduced wave equation in these coordinates is the familiar

$$[(r\partial_r)^2 + \partial_\theta^2 + r^2k^2]\Psi(r, \theta) = 0. \qquad (1)$$

It must be emphasized that we are looking at this equation with fresh eyes: we assume that it holds for ALL θ, not just those within a range of 2π, and that we do not restrict solutions by imposing the periodicity condition $\Psi(r, \theta + 2\pi) = \Psi(r, \theta)$. That is what is meant by the phrase *solutions in Polar Space*. We note that we might assume the stronger condition that the solution is an analytic function of θ for all complex values, but in this paper we only need it to be a continuous function of real values of θ. It will only be at a later stage, when we use the elementary polar solutions to build up to a solution to a physical problem, that we will end up with solutions which are periodic.

This paper will not deal with cases of oblique incidence, which is to say those cases in which the wave also has a harmonic dependence on Z, (the coordinate normal to the (r, θ)-plane) while the scattering object remains invariant under translation in the Z-direction. However we note that if the harmonic Z-dependence were $e^{ik_Z Z}$ then the same form of reduced wave equation is obtained with k^2 replaced by $k^2 - k_Z^2$. The same approach will therefore be applicable, though care must be taken in the case of electromagnetic waves where the boundary conditions complicate things and different polarization states have to be uncoupled [5].

We will be making extensive use of the following fundamental form of elementary solution to the polar wave equation:

$$\Psi(r, \theta) = \int_C F(z - \theta)e^{ikr\cos z}dz, \qquad (2)$$

where $F(z)$ is an analytic function of the complex variable $z = x + iy$. (Note that x and y will throughout the paper refer to this complex space and not to cartesian coordinates in physical space.) The contour of integration C is restricted only by the requirement that the integral converges. We will use the word *kernel* to refer to the function $F(z - \theta)$ and the phrase *exponential factor* to refer to $e^{ikr\cos z}$.

This general form of solution of the cylindrical wave equation is well-known and is commonly called the Sommerfeld integral. Much general detailed and precise work on this can be found in Budaev [10], and doubtless other texts. The point to bear in mind is that this paper does not for a moment claim that the use of integrals of this form is new: what is new is the way in which we obtain a solution which is a sum of such integrals, and, more importantly, where we do not stipulate that integral is a single valued function of position.

The most important characteristic of the exponential factor in this context is that it is exponentially small as $y \to +\infty$ provided $\sin x < 0$ and as $y \to -\infty$ provided $\sin x > 0$. Thus if we divide the z-plane into half strips by the lines $y = 0$ and $x = m\pi$, then we find that the exponential factor decays at infinity in half-strips alternating like the teeth of a zip fastener. In the upper half plane this means the strip $-\pi < x < 0$, repeated every 2π. In the lower half plane this means the strip $0 < x < \pi$, repeated every 2π. Let us for convenience name these half-strips the convergence strips. If the contour C extends to infinity then it MUST do so in one of the convergence strips for the integral to converge.

An important corollary of this is that in the convergence strips the exponential factor is an exponentially decaying function of r. That means that if the contour lies within (or can be continuously distorted into) a convergence strip then we automatically have an outgoing solution, as required for a scattered wave. The regions are illustrated in Fig. 1.

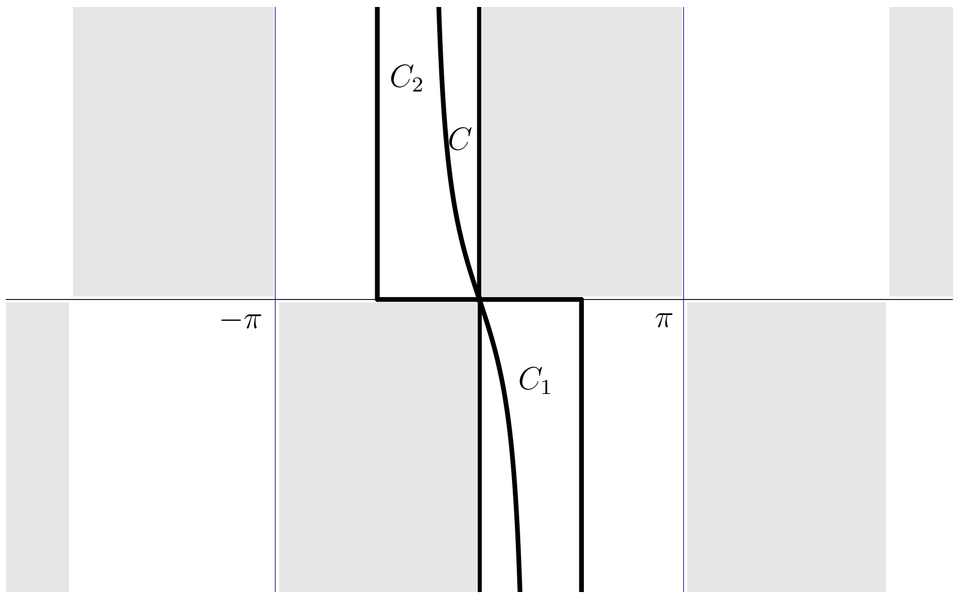

Fig. 1. Convergence strips (unshaded)with possible contours. C is the imaginary axis, C_1 is a generic symmetric contour, C_2 includes the sections C_-, C_+ with exponential decay (see text).

On the lines $C_- = (-\frac{1}{2}\pi, -\frac{1}{2}\pi + i\infty)$ and $C_+ = (\frac{1}{2}\pi, \frac{1}{2}\pi - i\infty)$ lying in the centers of their convergence strips the exponential decay is at its maximum and such contours may be thought of as part of a steepest descent contour. The same is true on lines displaced by 2π. These may have particular computational advantages, but theoretically *any* contour that has its ends running to infinity in the unshaded strips can be used. However, we will find it most useful to let our contour be $C = (-i\infty, i\infty)$ (with additions due to capture of poles and or branches which will be encountered later). The exponential term then has modulus unity on the whole contour and convergence depends on the behavior of $F(z - \theta)$. It is found in all the cases in this paper that this function decays at infinity sufficiently fast for convergence to be no problem.

In general we will find that the analytic kernel has singularities which may be poles or branch cuts. It should be noted that the pattern of singularities depends only on θ and not on r. As θ varies - and remember that θ is not limited to a total variation of 2π in our approach - the whole pattern of singularities moves to the right or left relative to the background of the convergence strips. Wherever we choose the contour of integration we will therefore find that for *some* values of θ a singularity will seem to lie on it. Using our fundamental assumption that the solution is a continuous function of θ except at boundaries in physical space, we will therefore follow the familiar path of distorting the contour of integration continuously to prevent a singularity actually crossing the contour.

Now this means that a part of the contour will be forced by the singularities of the kernel to move perhaps extensive distances parallel to the x-axis as θ varies. The crucial consequence is that a part of the contour will then be moved out of the convergence strips. Of course a finite displacement does not affect the *convergence* properties since the ends of the contour can continue to go to infinity within the strips. But it does make the corresponding component of the field an exponentially increasing function of r if the singularity lies definitely outside the convergence strips and an incoming wave if the singularity lies on some parts of the boundaries.

All approaches to scattering have to tackle the problem of how to separate the outgoing from the incoming solutions to obtain the physically significant one. In the present approach the problem is resolved by reference to the above remarks, a judicious choice of contour of integration, and use of the important fact that it does not matter if we use as a building block a term which is not outgoing for values of θ that will not appear in the final physical solution. It is quite easy to prove that (2) satisfies (1) provided that the integral converges and that the integrand takes the same value at either end of the contour, but we refer to the reader to other texts such as [10] for the details. It will be noticed that we also have solutions of the form (2), but with $F(z-\theta)$ replaced by $F(z+\theta)$. This turns out to be useful in what follows. Notice that if we have the former kernel then the pattern of singularities moves to the right against the background of the strips when θ increases, whereas the latter kernel leads to a pattern of singularities moving to the left.

We next look at a few special cases to illustrate and make familiar this approach. Suppose that $F(z)$ has a simple pole at $z = -\theta_0$, so that it has the form $F(z) = A(z)/(z + \theta_0)$ and suppose also that the contour C is a closed loop about the pole and does not contain any singularities of $A(z)$. Then the solution (2) reduces to

$$\Psi(r, \theta) = 2\pi i A(-\theta_0) e^{ikr\cos(\theta-\theta_0)}. \tag{3}$$

This represents a plane wave propagating in the direction $\theta = \theta_0$ with constant amplitude. It is also periodic in θ, a property that not all our solutions will share. This means that in fact it represents a plane wave which is incoming on multiple sheets. This type of term will arise frequently in our solution to real problems, but will there be restricted to certain regions of physical space.

Another case of special interest is that in which $F(z) = A$, a constant. If we then choose the contour C to be $(-i\infty, i\infty)$ then we find

$$\Psi(r, \theta) = A \int_{-i\infty}^{i\infty} e^{ikr\cos z} dz = -\pi A H_0^{(1)}(kr), \tag{4}$$

using known standard results [7], where $H_0^{(1)}(z)$ is a Hankel function. This is the field of a line source of magnitude $4\pi i A$ placed at the origin. It can be noted that we could have written C to be any contour with ends at $(-i\infty + x_1, i\infty - x_2)$, with $0 \leq x_i < \pi$ and have obtained the same result, as all such contours lie in the convergence strips and can be distorted (in the absence of any singularities in the integrand) into the one chosen.

It is natural to want to extend this result to cover the case in which there is a line source which is not at the origin. We begin with the more general question of changing the origin of our polar coordinate system to another point (r_0, θ_0). Let the polar coordinates of a field point (r, θ) relative to the new origin be (ρ, θ). Then

$$\rho e^{i\phi} = re^{i\theta} - r_0 e^{i\theta_0}. \tag{5}$$

Multiplication by a phase factor e^{iz} and then taking the real part gives

$$\rho\cos(z + \phi) = r\cos(z + \theta) - r_0\cos(z + \theta_0), \tag{6}$$

and hence, for any analytic function $F(z)$,

$$\int_C F(z) e^{ik\rho\cos(z+\phi)} dz = \int_C F(z) e^{ikr\cos(z+\theta)} e^{-ikr_0\cos(z+\theta_0)} dz. \tag{7}$$

We thus obtain the general result which enables us to transform our archetypal solution into one with polar coordinates but a different origin.

$$\int_{C_\phi} F(z-\phi)e^{ik\rho\cos z}dz = \int_{C_\theta} F(z-\theta)e^{-ikr_0\cos(z-\theta+\theta_0)}e^{ikr\cos z}dz. \tag{8}$$

Here the contours C_ϕ and C_θ are of course the contour C translated along the real axis by ϕ and θ respectively. In many cases they can be continuously deformed back into C without crossing any singularities or affecting convergence at infinity.

In the special case $F(z) = F_0$, a constant, then the left side of the above represents the field of a line source at $\rho = 0$. The right hand side then gives the same field, now represented in (r, θ) coordinates, with the source at (r_0, θ_0), as our archetypal form of solution with a kernel

$$G(z-\theta) = F_0 e^{-ikr_0\cos(z-\theta-\theta_0)}. \tag{9}$$

If it is desired, this may be combined with the result (4) to give

$$\int_{C_\theta} e^{-ikr_0\cos(z-\theta+\theta_0)}e^{ikr\cos z}dz = -\pi H_0^{(1)}(k\rho) \tag{10}$$

which may be known as another familiar way to transform from one coordinate system to the other.

In any case we can see how to deal, with no change in principle, with a problem involving the scattering of waves generated by a line source rather than scattering of a plane wave. This will, however, not be done in this paper, which will focus on the scattering of plane waves. We include the result to show how the current method can be extended to the more general case of a line source with only a small increase in complexity.

3 Elementary boundary conditions

We now use the general forms of solutions to satisfy a range of possible elementary boundary value problems. In this context the word *elementary* means that we are dealing with just one boundary at one value - ϕ - of θ. Such a problem is still non-physical. There is no such thing as a one-sided surface in physical space. Nevertheless these problems will be found to be the basis of a powerful method by which the solutions to real physical problems can be found as the sum of elementary solutions. At this stage, as in the case of the above plane wave, considerations of where exactly the solution is outgoing are not vital. Here we simply suppose a general incident field and present the basic calculations, deferring the question of the correct choice of contour to provide outgoing solutions in physical space until we reach that stage.

Problem 1. We look for a solution to the polar wave equation that satisfies the soft boundary condition: $\Psi(r, \phi) = 0$.

We at once see that a field of the form

$$\Psi(r, \theta) = \int_C [I(z - \theta) + R(z + \theta)]e^{ikr\cos z} dz \tag{11}$$

clearly satisfies our boundary condition provided

$$R(z + \phi) = -I(z - \phi). \tag{12}$$

So given an incident field with kernel $I(z)$ this result allows us to write down a corresponding reflected field with kernel $R(z)$. The process is very similar to that involved in solving the one-dimensional wave equation which has general solutions of the form $f(x \pm ct)$. Then we could construct solutions satisfying a boundary condition $\Psi(t, x_0) = 0$ in a precisely similar way: $\Psi(x, t) = I(x - ct) + R(x + ct)$, where $R(x_0 + ct) = -I(x_0 - ct)$. In short we are dealing at present with problems that are almost as simple as the one-dimensional wave equation! The only difference is that we are applying the algebra to a kernel and not the full solution.

Problem 2. Hard boundary condition: $\partial_\theta \Psi(r, \phi) = 0$.

The field (11) can be seen to satisfy this condition provided

$$R(z + \phi) = I(z - \phi). \tag{13}$$

Problem 3. Impedance boundary condition: $\partial_n \Psi(r, \phi) = i\beta\Psi(r, \phi)$.

Note that $\overrightarrow{n}$ is the direction of the normal *into* the surface and that then $\Re(\beta) > 0$ (assuming that we do not have an active surface that can amplify the waves). Then in the case that θ increases in the direction of the normal we find that equation (11) satisfies the boundary condition provided

$$(\sin z - \beta)R(z + \phi) = (\sin z + \beta)I(z - \phi), \tag{14}$$

or

$$R(z) = S(z)I(z-2\phi), \tag{15}$$

with

$$S(z) = \frac{\sin(z-\phi)+\beta}{\sin(z-\phi)-\beta}, \tag{16}$$

which reduces to the hard and soft cases as we let $|\beta| \to 0$ or $|\beta| \to \infty$ respectively. It will be noted that $S(z)$ has poles at $\sin(z-\phi) = \beta$. From the fact that $\Re(\beta) > 0$ we deduce that the roots must lie in the regions where $\sin(x-\phi) > 0$.

Problem 4. Refraction at material discontinuity.

This problem is significantly more complex than the earlier ones because we have two propagation constants, and in addition to a reflected field we have a refracted or transmitted wave. We label the media M_α with $\alpha = a, b$ where we will always suppose that the refractive index of M_b is greater than that of M_a. We label the corresponding propagation constants k_α and the fields as $\Psi_\alpha(r,\theta)$. The boundary conditions on an interface $\theta = \phi$ are the continuity of the field and the proportionality of their normal derivatives:

$$\Psi_a(r,\phi) = \Psi_b(r,\phi), \quad a\partial_\theta\Psi_a(r,\phi) = b\partial_\theta\Psi_b(r,\phi), \tag{17}$$

where a and b are constants depending on the properties of the materials, (and in the case of electromagnetic waves, on the polarization of the waves).

Now let us suppose that we have an incident and therefore also a reflected wave in medium M_a and a transmitted wave in medium M_b. Then with our now familiar integral representations of the fields we find that the first boundary condition has the form:

$$\int_D [I(z-\phi) + R(z+\phi)]e^{ik_a r\cos z}dz = \int_\Delta T(\zeta-\phi)e^{ik_b r\cos\zeta}d\zeta, \tag{18}$$

while for the second we require (after integration by parts)

$$ak_a\int_D [I(z-\phi) - R(z+\phi)]e^{ik_a r\cos z}\sin z dz = bk_b\int_\Delta T(\zeta-\phi)e^{ik_b r\cos\zeta}\sin\zeta d\zeta. \tag{19}$$

The integral in terms of ζ can be equated to that in terms of z via the key transformation

$$\cos z = n \cos \zeta \tag{20}$$

where $n = k_b/k_a$ is the refractive index of medium M_b relative to M_a (which by our convention must be greater than unity.) It follows from (20) that

$$\sin z dz = n \sin \zeta d\zeta. \tag{21}$$

This gives

$$\zeta'(z) = \frac{\sin z}{(n^2 - \cos^2 z)^{1/2}} \quad \text{and} \quad z'(\zeta) = \frac{n \sin \zeta}{(1 - n^2 \cos^2 \zeta)^{1/2}}. \tag{22}$$

Our essential requirement of the contours D and Δ is that they are connected by the key transformation. We will describe these after completing the algebra determining the kernels.

The boundary conditions become

$$\int_D [I(z-\phi) + R(z+\phi) - \zeta'(z)T(\zeta - \phi)]e^{ik_a r \cos z} dz = 0 \tag{23}$$

and

$$\int_D [I(z-\phi) - R(z+\phi) - \gamma T(\zeta - \phi)] \sin z e^{ik_a r \cos z} dz = 0 \tag{24}$$

where we have set $\gamma = b/a$. These will be satisfied if the kernels are identically zero, which simply requires

$$R(z+\phi) = \left(\frac{\zeta'(z) - \gamma}{\zeta'(z) + \gamma} \right) I(z-\phi) \tag{25}$$

and

$$T(\zeta(z) - \phi) = \left(\frac{2}{\zeta'(z) + \gamma} \right) I(z-\phi). \tag{26}$$

This last can more usefully be written

$$T(\zeta - \phi) = \left(\frac{2z'(\zeta)}{1 + \gamma z'(\zeta)} \right) I(z(\zeta) - \phi). \tag{27}$$

For scattering from medium M_b to M_a, with an incoming field having kernel $I(\zeta + \theta)$, we can write down the corresponding results by means of the transformations $z \leftrightarrow \zeta$ and $\gamma \leftrightarrow 1/\gamma$. We find

$$R(\zeta - \phi) = \left(\frac{\gamma z'(\zeta) - 1}{\gamma z'(\zeta) + 1} \right) I(\zeta + \phi) \tag{28}$$

and

$$T(z + \phi) = \left(\frac{2\gamma \zeta'(z)}{\gamma + \zeta'(z)} \right) I(\zeta(z) + \phi). \tag{29}$$

Having completed this simple algebra and formally derived the required kernels we next look in more detail at the contours D and Δ. It will be recalled that we need a one-to-one mapping of the one into the other under the transformation (20). Even a slight examination of this shows that it is not possible to make both contours lie along the imaginary axis, which was used in the earlier problems. Let us define the following quantities: $y_n = \cosh^{-1} n > 0$ and $\xi_n = \cos^{-1}(1/n) < 0$. We may then observe that the imaginary ζ-axis maps onto only that part of the imaginary z-axis which has $|\Im z| > y_n$. Equally the imaginary z-axis for which $|\Im z| < y_n$ maps into part of the real ζ-axis, between $\pm\xi_n$, the sign depending on a choice of branch. Consequently we need to think more deeply about exactly how to deal with the singularities and the contours.

We start by noting the precise positions of the branch points. The kernel $R(z + \theta)$, defined in (25), has branch points at $z_m^{\pm}(\theta) = -\theta + \phi - m\pi \pm iy_n$, with m any integer. The kernel $T(\zeta - \theta)$, defined in (27) has branch points at $\zeta_\mu^{\pm}(\theta) = \theta - \phi - \mu\pi \pm \xi_n$, with μ any integer. It will be noted that as we move away from the interface $\theta = \phi$, then the singularities of the respective functions in both the z and the ζ planes move to the right.

If we now look at the integral in medium M_a for a point very close to the interface then we find that the kernel $R(z + \theta)$ has singularities which lie just to the right of the imaginary axis, and so it seems to makes sense to let D continue to be the imaginary axis, as we have done in the other cases. For analyticity we can simply specify that, in the limit $\theta = \phi$, D must be moved slightly to the left of the singularities. This is illustrated in the first part of Fig. 2, in which the cuts are those which arise from taking the principle value of the root in $\zeta'(z)$: see equation (22). The second part of the figure gives the image Δ in the ζ-plane of that contour D, using $\zeta(z) = -\cos^{-1}(\cos z/n)$ and the principal value of this function. (Note the negative sign. This has been chosen so that the contour Δ tends to D in the limit $n \to 1$.) Now the process of fitting the boundary conditions imposes the restriction that when $\theta = \phi$ the contours D and Δ must be images of each other. The natural contour Δ

corresponding to the limiting contour D is then found to lie on the right of the cuts in the ζ-plane - pictured as the limit of the contour of Fig. 2.

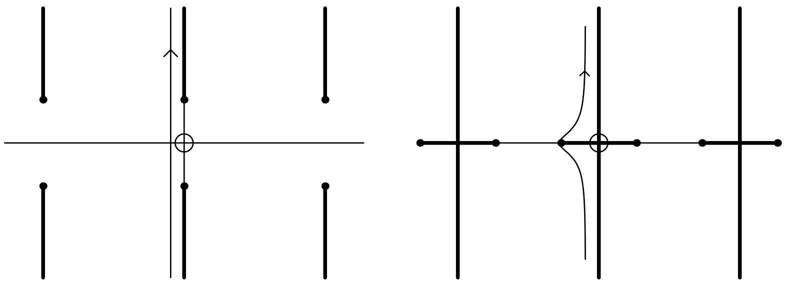

Fig. 2. Plausible integration contours in z-plane (left) and zeta-plane (right). The planes are cut to give the principle values to $\zeta(z)$ and $z(\zeta)$.

These contours will become the imaginary axis that we have used in other cases in the limit $n \to 1$, and at first sight it looks as if the slight distortion of the contour Δ about the part of the real axis between the origin and the branch point at $\zeta = -\xi_n$ - along which we cut the plane - is the only significant modification we require. Our physical intuition tells us that in the case of a material discontinuity we have the phenomenon of boundary waves. We connect boundary waves with branch point singularities. We are therefore not surprised to find some such modification.

However, if we look deeper, then we find that there are subtle problems which only arise as we move away from the interface. These problems have to do with the branch points. If we start by looking at the field in M_a, then we find that as θ moves away from the interface, all the branch points move right in the complex plane. That is fine up until $\theta = \phi - \pi$, and then the branch points at $z_1^{\pm}(\theta) = -\theta + \phi - \pi \pm i y_n$ reach the contour D. Of course the natural response to this is simply to distort the contour to the right, to preserve continuity. BUT, and here is the problem, this involves moving the contour about the upper branch point into a semi-strip in the z-plane in which the corresponding field is exponentially increasing with r. This would not give a physical, outgoing, solution.

However, a little thought shows that we can compensate for this by adding to our contour D an additional loop about a branch cut upwards from $z_1^{+}(\theta)$, when it lies in the third quadrant, as illustrated in Fig. 3. When θ passes through $\phi - \pi$ this cut crosses the imaginary axis and loses its loop in the usual way. However at this same stage the cut from $z_1^{-}(\theta)$ also crosses the imaginary axis and acquires a loop. This is also shown in Fig. 3.

With these additions we have a solution which consists of a line integral together with an integral along a cut which lies in an unshaded, or convergent, strip as long as $\theta > \phi - 2\pi$. Now for our purposes that would seem to be enough. It means that we have a solution that is analytic and well-behaved

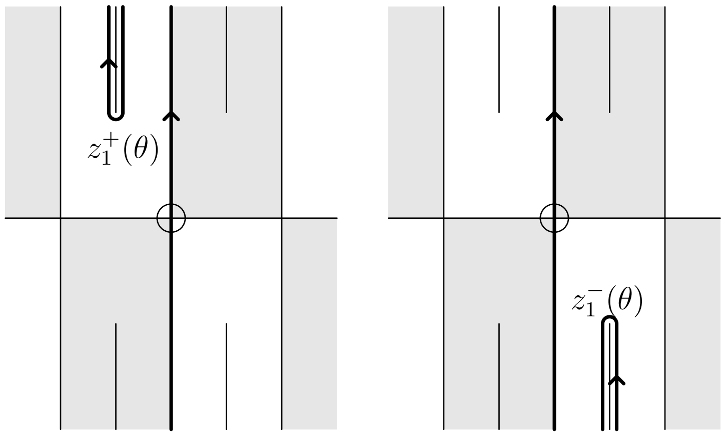

Fig. 3. Integration contours in z-plane for $\phi > \theta > \phi - \pi$ (left) and $\phi - \pi > \theta > \phi - 2\pi$ (right).

for a range of 2π, and that is all we will need when we come to applying this partial solution to built a solution to a physical problem by iteration, as will perhaps be more clear later.

The purist will, however, naturally wonder if it is possible to generate a solution to the current, non-physical, problem for a yet wider range of θ. So let us continue, analytically, to let θ drop into the range $\phi - 2\pi > \theta > \phi - 3/\pi$. In the process the branch cuts from $z_2^+(\theta)$ and $z_1^-(\theta)$ both move into shaded strips, which will mean that they will give exponentially increasing contributions. How can this be prevented? By adding more vertical contours at $x = \pm\pi$, running in the opposite direction to our primary line contour. Of course, once we have started on this path, we naturally wish to extend it to further values of θ and this quickly leads us to arrive at the infinite set of contours, which we will call D_∞, shown in Fig. 4.

In the figure we have assumed that $\phi > \theta > \phi - \pi$, as is indicated by the labelled branch cuts. But as θ decreases we find that as the branch cuts pass through the vertical contours they shed their loops as they move into the shaded regions or acquire them as they pass out of the shaded regions. In this way we can ensure that the integrals remain convergent for all values of θ in the medium M_a. This formally solves the problem of finding a solution throughout the nonphysical space, but we do not see at present any practical need for this solution.

We next turn to the question of the contour Δ that corresponds to the modified form of D. We start with the form that arises when we take D to be the slightly modified contour of Fig. 3. This is shown in Fig. 5. Here we have placed the cuts in the ζ-plane to run vertically, which makes them more similar to those in the z-plane. This transforms the contour shown in Fig. 2 into a contour along the imaginary axis and a loop upwards along a cut. The other vertical

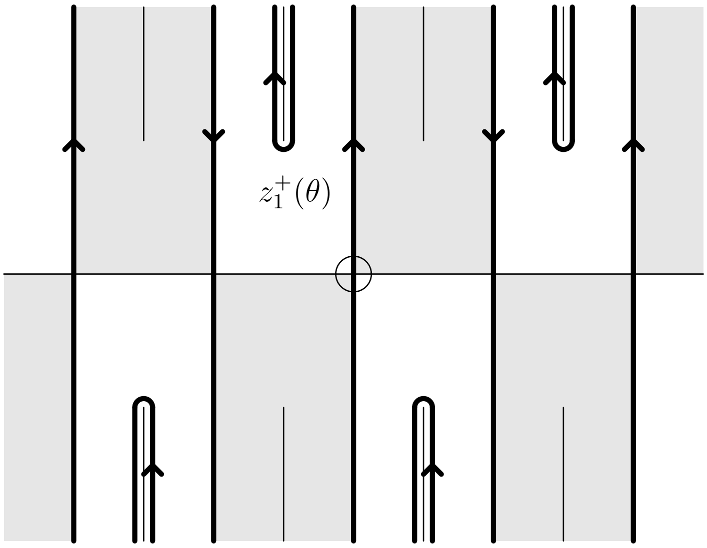

Fig. 4. Complete integration contours D_∞ in z-plane for $\phi > \theta > \phi - \pi$. The patterns remains essentially the same for *all* $\theta < \phi$.

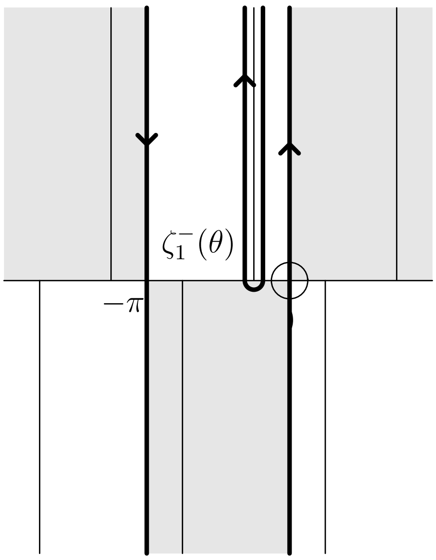

Fig. 5. Modified integration contour in zeta-plane for angle close to interface, with cuts vertical.

contour though $\xi = -\pi$ is the image of the loop contribution to D in the z-plane.

This contour is sufficient for many purposes. It runs into trouble only when $\zeta_1^-(\theta)$ increases to π, when the loop which the cut picks up when it passes the contour on the imaginary axis, and reaches the shaded strip beyond $\xi = \pi$. In cases where the wedge is made of the material M_b this will never happen and we can therefore use the simple contour above. However we can proceed to generalize to wider ranges of θ as we did in the case of D if it should be required, if necessary to the point of finding a form valid for an infinite range of θ, which is illustrated in Fig. 6.

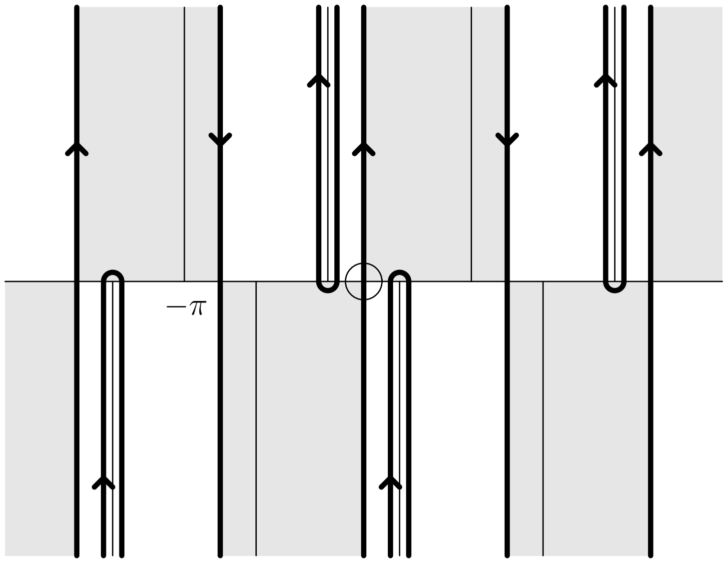

Fig. 6. Modified integration contour Δ_∞ in zeta-plane, valid for all angles θ.

The two patterns of contours D_∞ and Δ_∞ are very similar in general form, which is satisfactory. It will be recalled that they only have to be exact images of each other when $\theta = \phi$, for purposes of fitting the boundary conditions, and only then. For other values the forms are restricted only by the condition of continuity in θ and can be moved, consistently with that, to positions which are convenient for computation. However in this paper we will in practice only ever be using the simpler contours of Figs. 3 and 5, and using them to build up an iterated solution to scattering by a wedge, where we never need a solution with a range of θ greater than 2π. This will become more clear as the paper develops.

4 Scattering by a line singularity

We now move from the above general solutions, which can be applied in a variety of contexts, and with a variety of kernels and contours and deal with the specific example which is of central importance. Our primary objective here can be stated as obtaining a solution to the wave equation in Polar Space which represents a plane incoming wave scattered by a line singularity. An intermediate step is to find a solution that models a shadow boundary.

We start by considering the following simple example of our fundamental integral form, in which we take the contour of integration to be the imaginary axis and the kernel to have a simple pole:

$$\Psi(r,\theta) = \frac{1}{2\pi i} \int_{-i\infty}^{i\infty} \frac{1}{z-\theta+\theta_0} e^{ikr\cos z} dz. \tag{30}$$

Now this solution, as written, has a discontinuity at $\theta = \theta_0$, which is contrary to our basic assumption that the field must be a continuous function of θ. However this is easily corrected by specifying that the contour of integration is distorted continuously as θ passes through θ_0. This gives rise to an additional contour consisting of a small circle about the pole.

Thus if we suppose that the field $\Psi(r,\theta)$ is given by the above line integral when $\theta > \theta_0$, then it will be given by a line integral plus a circular contour when $\theta < \theta_0$. These contours are shown in Fig. 7 and the corresponding mathematical representation is

$$\Psi(r,\theta) = -H(\theta_0-\theta)e^{ikr\cos(\theta-\theta_0)} + \frac{1}{2\pi i} \int_{-i\infty}^{i\infty} \frac{1}{z-\theta+\theta_0} e^{ikr\cos z} dz, \tag{31}$$

which represents a plane wave in $\theta > \theta_0$ together with an outgoing cylindrical wave.

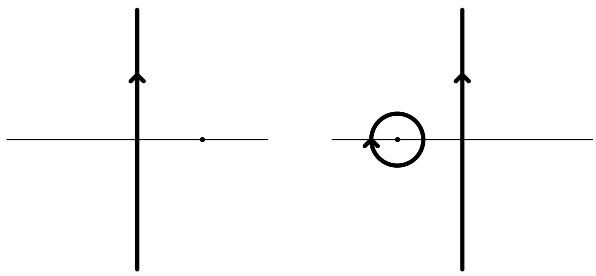

Fig. 7. Contours with $\theta - \theta_0 > 0$ and $\theta - \theta_0 < 0$.

This key result gives us the power smoothly to model a shadow boundary. The drawback is that although the line integral represents an outgoing wave the plane wave is outgoing for some values of θ and incoming for others relative to the origin. However this problem can be corrected quite easily, by a method similar to indicated at the end of the previous section. We can simply introduce another line integral displaced by 2π from our first, so that the total solution consists of the line integrals together with a circle about the pole when it lies between them, and only then. Alternatively we can combine the two integrals into one and, after adding an incoming wave, we can write down the solution to the scattering of a plane wave by a line singularity in the more convenient form:

$$\Psi(r,\theta) = \Psi_I(r,\theta)H(\pi - |\theta - \theta_I|) + \int_{-i\infty}^{i\infty} \frac{-i}{(z-\theta+\theta_I)^2 - \pi^2)} e^{ikr\cos z} dz. (32)$$

where Ψ_I is a plane wave of unit magnitude:

$$\Psi_I(r,\theta) = e^{-ikr\cos(\theta-\theta_I)}. \quad (33)$$

Notice that to make use of a certain symmetry we have chosen the angle θ_I to be the direction from which the plane incident wave Ψ_I is *coming*.

When $|\theta - \theta_I| < \pi$ then the kernel of the line integral has one pole on either side of the contour. As θ moves out of this range then one or other pole crosses the contour. In doing so it picks up a contour which gives a term which exactly cancels the incident wave. It thus models the shadow boundaries.

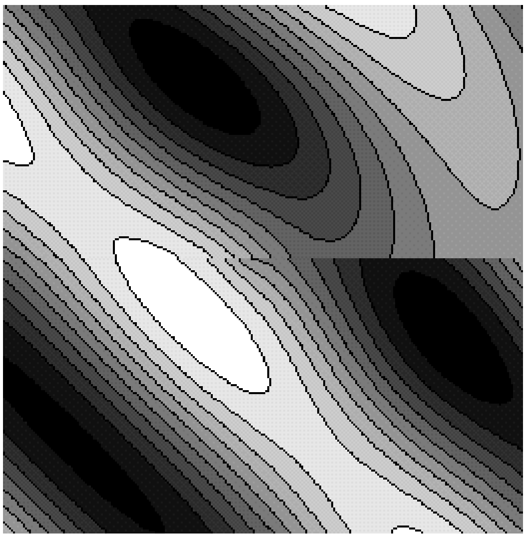

Fig. 8. Wave diffracted by a line singularity in one sheet of Polar Space.

We present in Fig. 8 a contour plot of this wave pattern produced by Mathematica. Of course we cannot show the field for all values of θ and have simply shown it on one sheet $0 < \theta < 2\pi$, which is why there appears to be a discontinuity at $\theta = 0$ or $\theta = 2\pi$. It shows an incident field from the bottom left being diffracted smoothly around the origin. *This basic modification of the incident plane wave in Polar Space, which takes account of scattering by the edge will be the basis of all that follows.*

5 Semi-infinite sheet

Next we come to the first of a series of problems in physical as opposed to Polar Space. In these we will be using the above elementary results to build up a solution in an iterative way which will be found to have definite virtues.

In this section we treat a well-known problem, that of scattering by a semi-infinite sheet. This is normally done by the equally well-known Wiener-Hopf technique, e.g. Jones[7], but we here show how it can be solved precisely by the different and simpler method of the current paper, and also later explore the accuracy of simple approximate solutions that this method can also provide.

We will suppose that the sheet's top surface is $\theta = 0$ and that the bottom surface is $\theta = 2\pi$. We will suppose an incident plane wave which *comes from* the direction $\theta = \theta_I$, with $0 < \theta_I < 2\pi$. To begin with we will solve, with details of the process, the case in which the boundary conditions on both surfaces are soft, i.e. $\Psi = 0$. Other cases will then be treated without the need for so much detail.

Now in order to obtain the correct behaviour at the shadow boundaries we have seen that it is necessary to replace the incident plane wave by the form (32) which also contains the cylindrical scattered field with kernel

$$K_0(z-\theta) = \frac{-i}{(z-\theta+\theta_I)^2-\pi^2} \tag{34}$$

Of course this term will not satisfy the boundary conditions, but it is an elementary matter, using the results of section 2, to add to it terms which will correct this.

Thus the first iteration will require the kernel

$$K_1(z+\theta) = \frac{i}{(z+\theta+\theta_I)^2-\pi^2} \tag{35}$$

which will, when added to K_0, exactly fit the boundary condition at $\theta = 0$, and likewise

$$K_2(z+\theta) = \frac{i}{(z+\theta-4\pi+\theta_I)^2-\pi^2} \tag{36}$$

will similarly cancel K_0 on $\theta = 2\pi$. Of course K_1 does not satisfy the boundary condition on $\theta = 2\pi$ and has to be balanced by another term

$$K_3(z-\theta) = \frac{-i}{(z-\theta+4\pi+\theta_I)^2-\pi^2}. \tag{37}$$

Similarly K_2 does not satisfy the boundary condition on $\theta = 0$ and has to be balanced by another term

$$K_4(z-\theta) = \frac{-i}{(z-\theta-4\pi+\theta_I)^2-\pi^2}, \tag{38}$$

and so on.

It is then quite easy to see that by continuing the process we will have a kernel

$$K_{ss}(z,\theta) = \sum_{m=-\infty}^{\infty} \frac{-i}{(z-\theta+4m\pi+\theta_I)^2-\pi^2} - \frac{-i}{(z+\theta+4m\pi+\theta_I)^2-\pi^2}. \tag{39}$$

If there is any doubt, then a simple inspection of this form is enough to verify that it satisfies the boundary conditions.

Now there is an identity, which is proved in Appendix A, that

$$2\pi \sum_{m=-\infty}^{\infty} \frac{1}{(z+4m\pi)^2-\pi^2)} = -\frac{1}{2}\sec\frac{z}{2}, \tag{40}$$

consequently

$$K_{ss}(z,\theta) = \frac{i}{4\pi}(\sec\frac{z-\theta+\theta_I}{2} - \sec\frac{z+\theta+\theta_I}{2}). \tag{41}$$

It is immediately verifiable that this satisfies the boundary conditions.

We now need simply to tie up one last detail, which has to do with the treatment of specularly reflected waves. It will be noted that the kernel that we have generated iteratively has poles at $z - \theta + \theta_I - 4m\pi = \pm\pi$ and $z + \theta + \theta_I - 4m\pi = \pm\pi$. We need to know if these ever lie on the contour of integration, for we have seen above how such conditions model shadow boundaries. For physical values of θ and θ_I (between 0 and 2π) the only poles of the first set that can cross the contours are at $\theta = \theta_I \pm \pi$. These are the shadow boundaries that we have already dealt with. The shadow boundaries from the second set lie at $\theta + \theta_I - 4m\pi = \pm\pi$. If $\theta_I < \pi$ this gives $\theta = \pi - \theta_I$. If $\theta_I > \pi$ we instead find $\theta = 3\pi - \theta_I$.

We thus find that the full solution to this problem is

$$\Psi_{ss}(r,\theta) = \Psi_I(r,\theta)H(\pi - |\theta-\theta_I|) + \Psi_R(r,\theta) + \int_{-i\infty}^{i\infty} K_{ss}(z,\theta)e^{ikr\cos z}dz, \quad (42)$$

where Ψ_R gives the specularly reflected components

$$\Psi_R(r,\theta) = -(H(\pi-\theta_I-\theta)H(\pi-\theta_I) + H(\theta-3\pi+\theta_I)H(\theta_I-\pi))e^{-ikr\cos(\theta+\theta_I)}. \quad (43)$$

These components, as expected, come *from* the direction $\theta = -\theta_I$ and inspection verifies that they are in the regions that physical intuition suggests.

In a similar way we can write down, with the aid of the result of problem 2 of section 2 the kernel when the boundary condition on both sides of the plane are hard. It is

$$K_{hh}(z,\theta) = \sum_{m=-\infty}^{\infty} \frac{-i}{(z-\theta-4m\pi+\theta_I)^2-\pi^2} + \frac{-i}{(z+\theta-4m\pi+\theta_I)^2-\pi^2}, \quad (44)$$

which is summed in the same way to

$$K_{hh}(z,\theta) = \frac{i}{4\pi}(\sec\frac{z-\theta+\theta_I}{2} + \sec\frac{z+\theta+\theta_I}{2}). \quad (45)$$

We can also write down the solution to the problem in which the top surface is soft and the bottom is hard. The only difference is in the signs of some terms, and it is easily shown that

$$K_{sh}(z,\theta) = \sum_{m=-\infty}^{\infty} \frac{-i(-1)^m}{(z-\theta-4m\pi+\theta_I)^2-\pi^2} - \frac{-i(-1)^m}{(z+\theta-4m\pi+\theta_I)^2-\pi^2}, \quad (46)$$

which can also be summed, using results from Appendix A to give

$$K_{sh}(z,\theta) = -i\csc\left(\frac{z-\theta+\theta_I}{4}\right). \quad (47)$$

Note that our claim is that this method of tackling the problem is conceptually simpler than the Weiner-Hopf method. It could be taught to and understood by a student with far less effort. We are, of course, not saying that the results in themselves are new, although a small amount of manipulation is required to change the form which arises naturally in this approach into the form that arises most naturally by the earlier standard method. However there is an additional attraction, which is that it yields approximate solutions with minimal work. We next explore this.

6 The accuracy of a truncated series

In this section we will look at the question of the amount of error involved in approximating the correct scattered field by a truncated series. We will do this for the problem with soft boundary conditions to illustrate and illuminate. We will thus be comparing an exact expression like

$$\Psi(z,\theta) = \frac{i}{4\pi} \int_{-\infty}^{\infty} \left(\sec\frac{z-\theta+\theta_I}{2} - \sec\frac{z+\theta+\theta_I}{2} \right) e^{ikr\cos z} dz \tag{48}$$

and a truncated approximation, which will to some extent be chosen with reference to where the estimate is being made.

Thus suppose that we have a wave incident on the semi-infinite sheet from below. It is clear that in the fully illuminated region the magnitude of the cylindrically scattered field will in practice be of quite small significance compared with the incident field. By contrast in the shadow region above the sheet the cylindrical field is the whole field and so it becomes a matter of great interest to compare an approximation with the true solution.

One measure of the accuracy can be obtained by considering the proportional error between the true cylindrical field and the approximate cylindrical field in that region:

$$\text{Error} = |\Psi - \Psi_A| / |\Psi|. \tag{49}$$

Alternatively we can consider the absolute error, relative to the magnitude of the incoming field (which is unity):

$$\text{AbsError} = |\Psi - \Psi_A|. \tag{50}$$

The first approximate field is one which includes the first order correction with kernel K_1, which takes account of the boundary condition on the shadow side of the contour:

$$\Psi_1(z,\theta) = \int_{-\infty}^{\infty} (I(z-\theta) - I(z+\theta)) e^{ikr\cos z} dz, \tag{51}$$

where the kernel is the familiar function

$$I(z) = \frac{-i}{(z+\theta_I)^2 - \pi^2}. \tag{52}$$

Of course this must be quite approximate as it will be the same whatever the boundary condition on the lower face of the sheet. We might intuitively expect it to be reasonable away from the edge but poorer near the edge where the nature of the lower surface will have more effect. To adjust for this we can include kernel $K_2 = I(z+\theta-4\pi)$ obtained by meeting the conditions on the lower surface and the kernel $K_3 = I(z-\theta-2\pi)$ which will cancel K_2 on the top surface. Thus

$$\Psi_2(z,\theta) = \int_{-\infty}^{\infty} (I(z-\theta) - I(z+\theta) - I(z+\theta-4\pi) + I(z-\theta-4\pi))e^{ikr\cos z}dz. \tag{53}$$

(Inspection verifies that this satisfies the soft boundary condition on $\theta = 0$.)

It is clear that it is the simplest of matters to add further terms if we are looking for higher accuracy - it would be child's play for a computer to add a dozen or more terms to the above truncated kernel with very little cost in computing time. However we are here going to show that for most practical purposes it is scarcely necessary to go any further.

Fig. 9 shows the absolute error functions plotted $0 \leq \theta \leq \pi/2$ and for a range of kr over four orders of magnitude and for a plane wave normally incident on the sheet from below ($\theta_I = 3\pi/2$). The dotted curve gives the absolute error of Ψ_1 and the solid line gives the absolute error of Ψ_2. It will be seen that even the first order approximation is in error by an amount that is of the order of 1% of the incident wave or less, and the second order approximation is of the order of 0.1% of the incident wave. There seems no reason why any higher accuracy would be of value in the real world.

We also show the error of the approximations relative to the scattered field in Fig. 10. Here we find that the first order approximation can be in error by up to 10% proportional to the scattered field, which may be large by mathematical standards but is not large in practical terms where a simple, good order of magnitude estimate can be invaluable. This error is not so surprising since this level of approximation takes no account of the material of the lower surface. However the minimal extra work involved in going to the second order approximation (the first which also takes account of the lower face) brings the relative error down to the 1% mark which must be good enough for any practical purposes.

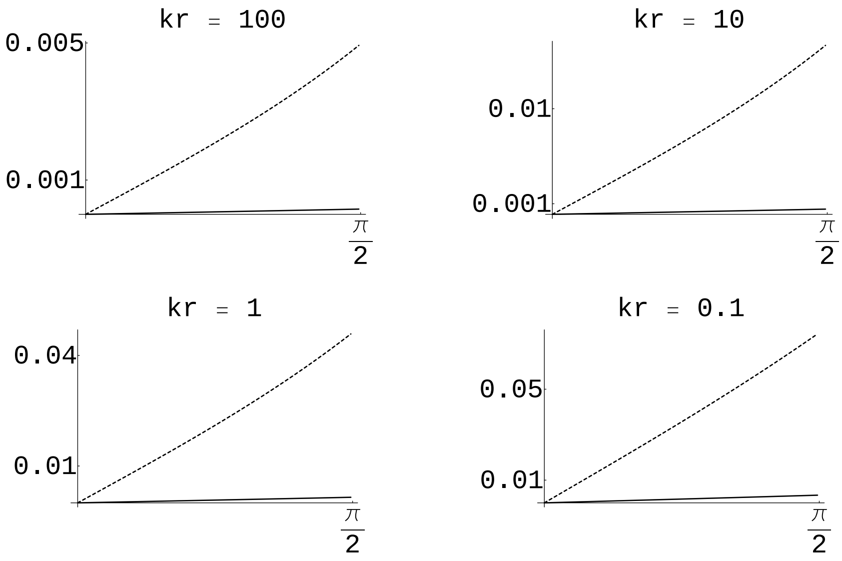

Fig. 9. Absolute error of scattered field with first (dashed) and second approximation, plotted for $0 \leq \theta \leq \pi/2$.

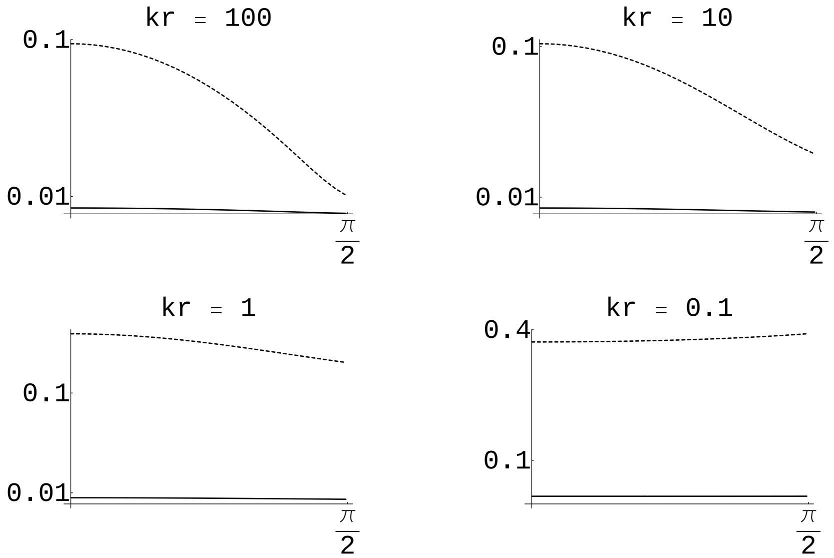

Fig. 10. Relative error of scattered field with first (dashed) and second approximation, plotted for $0 \leq \theta \leq \pi/2$.

We cannot emphasize too much how remarkable this result is from the point of view of engineers. Errors of that magnitude are totally negligible since they will be swamped by a multitude of other factors that arise from such things as the impossibility of achieving perfectly soft boundary condition, perfectly thin sheets, a perfectly non-reflecting environments etc., etc. These calculations show that as a result of some very simple algebra and one numerical integration we obtain answers to all questions about the field scattered by edges with an accuracy more than ample for all practical purposes. When we add the fact that we can use the same method with but little modification to deal with wedges and with mixed and impedance boundary conditions we have overwhelming reasons why this new method is of value.

We will not overburden this paper with graphs of the various possible configurations of incident wave direction, boundary conditions and angles of wedges, which could be churned out by the hundred. The purpose of the paper is to describe a new tool and to indicate its probable value. Extensive use of it will come later.

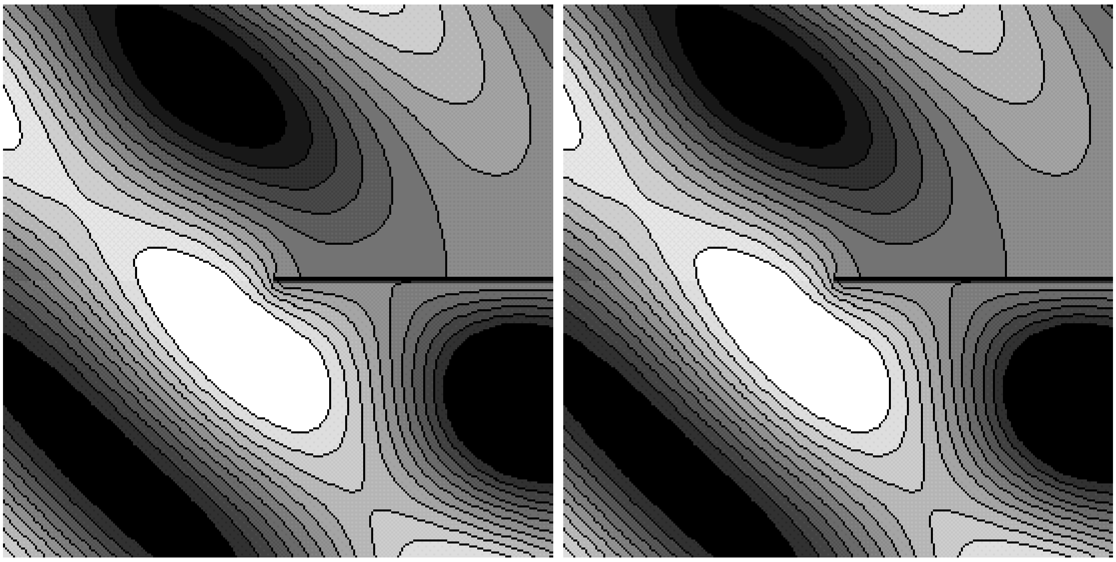

Fig. 11. Field scattered by a soft edge with exact (left) and approximate (right) kernels.

We simply show in Fig. 11 a contour plot of the amplitudes calculated for the field scattered by a semi-infinite sheet with soft boundary conditions using the exact and the approximate kernels. The visual impact of this, we suggest, reinforces our contention that the approximate kernel gives remarkably good results. It is clear that the contour lines of a given amplitude are but very little displaced, so much so that it requires some minutes of close study to find any differences with the naked eye. That is what a 1% error looks like.

7 Diffraction by impermeable wedges.

Next we show that another virtue of this approach is that it treats scattering by wedges with hard or soft boundary conditions quite as easily *and by the same method* as it dealt with the semi-infinite plate. This should be contrasted with the fact that previous approaches have involved totally different methods which are mathematically more abstruse, harder to learn and difficult to apply.

We will suppose that the top surface of the wedge is at $\theta = \phi_1$ and the bottom at $\theta = \phi_2 > \phi_1$. We will also move on to the more general case of assuming mixed or impedance boundary conditions. This means that

$$\partial_\theta \Psi(r, \phi_1) = -ikr\beta_1 \Psi(r, \phi_1), \; \partial_\theta \Psi(r, \phi_2) = ikr\beta_1 \Psi(r, \phi_2), \tag{54}$$

where $\Re\beta_i > 0$. We can regain the soft or hard conditions by letting $\beta_i = 0$ or $\beta_i \to \infty$ respectively.

We can start, as usual, with the kernel that simply models scattering by the line of the edge, and then iterate by fitting the boundary conditions on the faces as above. However with only a little experience the general form of the series thus obtained becomes clear and it is simpler just to work from this form. In essence we find that successive iterates have kernels with arguments $z - \theta$ and $z + \theta$ alternating and with a change of phase at each step. At a first reading it may be worth writing down the first few terms as we did in the last section for familiarization, but we here write down the general form directly:

$$K(z, \theta) = \sum_{m=-\infty}^{\infty} G_m(z - \theta) + H_m(z + \theta) \tag{55}$$

where

$$G_m(z) = g_m(z) I(z - m\Phi), \;\; H_m(z) = h_m(z) I(z - 2\phi_1 - m\Phi), \tag{56}$$

$g_0 = 1$, $I(z)$ is the familiar

$$I(z) = \frac{-i}{(z + \theta_I)^2 - \pi^2}, \tag{57}$$

and

$$\Phi = \phi_2 - \phi_1 \tag{58}$$

is 2π less the angle of the wedge. It reduces to 2π therefore for the limiting case of a sheet.

Using the results of problem 4 of section 2 we see that this will satisfy the boundary condition on $\theta = \phi_1$ provided that

$$\sum_{m=-\infty}^{\infty} (\sin z - \beta_1) g_m(z - \phi_1) I(z - \phi_1 - m\Phi) =$$

$$\sum_{m=-\infty}^{\infty} (\sin z + \beta_1) h_m(z + \phi_1) I(z - \phi_1 - m\Phi), \tag{59}$$

which will be true if

$$(\sin z - \beta_1) g_m(z - \phi_1) = (\sin z + \beta_1) h_m(z + \phi_1). \tag{60}$$

The boundary condition on the lower face will be satisfied if

$$\sum_{m=-\infty}^{\infty} (\sin z + \beta_2) g_m(z - \phi_2) I(z - \phi_2 - m\Phi) = \\ \sum_{m=-\infty}^{\infty} (\sin z - \beta_2) h_m(z + \phi_2) I(z + \phi_2 - 2\phi_1 - m\Phi). \tag{61}$$

Noting that $I(z + \phi_2 - 2\phi_1 - m\Phi) = I(z - \phi_1 - (m-1)\Phi)$ we see that the above will hold if

$$(\sin z + \beta_2) g_m(z - \phi_2) = (\sin z - \beta_2) h_{m+1}(z + \phi_2). \tag{62}$$

The equations (60) and (62) allow us to generate all the terms of the series in a straightforward way. And for a computer evaluation of the fields this can be regarded as sufficient. However for analytic purposes it may be worth manipulating these forms into other, simpler ones.

We start by eliminating g_m to give

$$\frac{\sin(z + \phi_1) + \beta_1}{\sin(z + \phi_1) - \beta_1} h_m(z + 2\phi_1) = \frac{\sin(z + \phi_2) - \beta_2}{\sin(z + \phi_2) + \beta_2} h_{m+1}(z + 2\phi_2) \tag{63}$$

which can be written more symmetrically as

$$\frac{\sin(z - \phi_2) + \beta_1}{\sin(z - \phi_2) - \beta_1} h_m(z - \Phi) = \frac{\sin(z - \phi_1) - \beta_2}{\sin(z - \phi_1) + \beta_2} h_{m+1}(z + \Phi). \tag{64}$$

We therefore write

$$F_1(z) = \frac{\sin(z - \phi_2) + \beta_1}{\sin(z - \phi_2) - \beta_1}, \quad F_2(z) = \frac{\sin(z - \phi_1) + \beta_2}{\sin(z - \phi_1) - \beta_2}, \tag{65}$$

and define

$$F(z) = F_1(z) F_2(z). \tag{66}$$

It is then possible to write down the iteration formulae

$$g_{m+1}(z+\Phi) = F(z)g_m(z-\Phi), \quad h_{m+1}(z+\Phi) = F(z)h_m(z-\Phi), \tag{67}$$

the latter following in virtue of (60). Since $g_0(z) = 1$ and, as a simple consequence

$$h_0(z) = F_1^{-1}(z+\Phi) \;\; h_1(z) = F_2(z-\Phi), \tag{68}$$

there is no problem in principle of solving these equations numerically.

We dispose first of the cases in which the surfaces of the wedge are hard and/or soft. We notice that if a surface S_i is soft so that $\beta_i = 0$, we find $F_i(z) = 1$. Similarly if S_i is hard so that $\beta_i = \infty$ we find $F_i = -1$. These clearly simplify the iterative equations considerably since we have either $F(z) = 1$ if both faces are hard or both soft, or $F(z) = -1$ if one is hard and one soft. We thus regain quite simply the general forms of solutions of the last section. The only difference lies in the fact that we are here dealing with a wedge and not an edge, which is to say with general Φ and not 2π. There is no virtue in writing down all the various combinations of hard and soft again. We simply note that equation (69) now becomes

$$K_{ss}(z,\theta) = \sum_{m=-\infty}^{\infty} \frac{i}{(z-\theta+2m\Phi+\theta_I)^2-\pi^2} - \frac{i}{(z+\theta+2m\Phi+\theta_I)^2-\pi^2}. \tag{69}$$

and so (41) becomes

$$\begin{aligned} K_{ss}(z,\theta) = \frac{i}{2\pi}\lambda(&\cot\lambda(z-\theta+\theta_I-\pi) - \cot\lambda(z-\theta+\theta_I+\pi) \\ &- \cot\lambda(z+\theta+\theta_I-\pi) + \cot\lambda(z+\theta+\theta_I+\pi)), \end{aligned} \tag{70}$$

where $\lambda = \pi/2\Psi$. The kernels for the other boundary conditions being hard and/or soft can be written down in a similar manner with little difficulty.

In the more difficult case of impedance boundary conditions it is impossible to sum the series, but we will briefly show how to evaluate any order of kernel. We see that since $g_0 = 1$, $g_1(z) = F(z-\Phi)$, $g_2(z) = F(z-\Phi)g_1(z-2\Phi)$, and so $g_2(z) = F(z-\Phi)F(z-3\Phi)$, etc. and generally, for $m > 0$

$$g_m(z) = \prod_{j=1}^{m} F(z-(2j-1)\Phi)). \tag{71}$$

When $m < 0$ we use

$$g_{m-1} = F^{-1}(z) g_m(z + \Phi) \tag{72}$$

and then find similarly

$$g_{-|m|}(z) = \prod_{j=1}^{|m|} F^{-1}(z + (2j-1)\Phi). \tag{73}$$

It is then a matter of turning to a computer to evaluate as many terms of the expansion as are necessary for a given purpose. We argue that the evidence of the earlier comparisons suggests that for most purposes only a few terms would be needed. A full comparison with known solutions (cf. [4]), which themselves involve considerable computational complexity, would take us too far away from the main purpose of this paper which is to demonstrate the principles and relative simplicity of the approach.

8 Diffraction by permeable wedges

We now see bring this iterative technique to bear on a problem that has proved to be remarkably difficult and to date has no theoretical method of solution. It is the case of a plane wave diffracted by a permeable wedge. In the case of electromagnetic waves it will often be called a dielectric wedge. It may be worth bearing in mind in what follows the common school-child experiment of passing a beam of light through a glass prism. A narrow beam follows the trajectory of a ray in the ray optics approximation. We typically notice a series refractions and reflections at the faces of the prism, though the dominant effect is just light refracted at the first and second faces as it passes through. There are in fact multiple internal reflections but in general all but the primary ones are small enough to be neglected for practical purposes. A low order ray optics approximation to this situation is outlined in Fig. 12. It shows the first three shadow boundaries outside the prism, one from the incident wave, one from the wave reflected from the first (lower) face, and one from the primary wave refracted by the second face in the region above the prism. Of course it assumes that the angle of incidence is such that there *is* a plane refracted wave at the second surface, and not a totally internally reflected wave. Although such considerations make for a certain complexity in writing down the terms of a ray optics solution, they do not give any problem *in principle*. We will find that something similar can be said about our general wave solution.

It is intuitively clear that a full solution to this problem, even at the ray optics

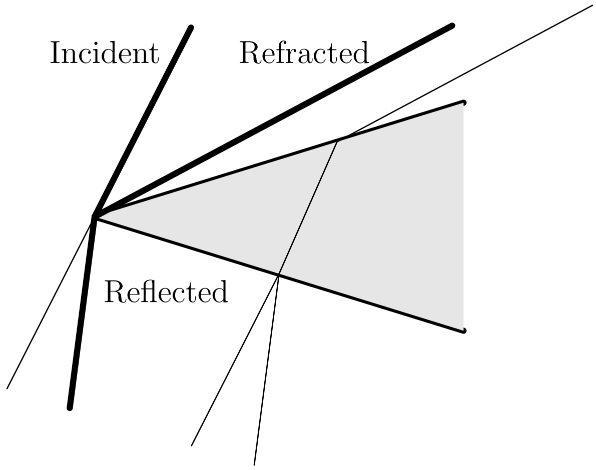

Fig. 12. The path of a ray passing through a wedge and the path of a ray passing through the vertex, showing the shadow boundaries of the incident, reflected and refracted waves.

level, will be considerably more difficult than the earlier problems covered in this paper. For one thing there will in general be multiple internal reflections. Once we move from the ray optics approximation it is a well-known fact that the difference in refractive index of the two media gives rise to such phenomena as total internal reflection and boundary waves, all of which can be expected to be represented by the mathematics of the solution. It is therefore perhaps not surprising that the analytic solution to the problem of scattering by a dielectric wedge has historically proved remarkably intransigent.

However we will show in this section how our iterative approach to scattering by wedges can be applied to this class of problems. The conception is identical to that used in the earlier sections. The details, inevitably, show more complexity. However we can again show that the solution can be represented as an infinite sum of integrals, each of which has a kernel which can be derived algebraically from the kernel of the previous one.

For didactic purposes we start *not* by leaping immediately into the integrals of the iterative solution which can conceal the conceptual simplicity of the approach. Instead we will take the intermediate step of first calculating some coefficients of the ray optics approximation *in the coordinate system that we are using*. These are in fact closely related to the kernels which we will later be using. But for anyone who is not too familiar with this area it may well make things easier to grasp.

8.1 *Ray optics terms*

The lowest order ray optics term is an incoming plane wave with its shadow boundaries.

$$\Psi_0^{ray}(r,\theta) = e^{ikr\cos(\theta-\theta_I+\pi)}H(\pi - |\theta - \theta_I|), \tag{74}$$

though of course in the particular configuration illustrated in Fig. 12 only the one shadow boundary is relevant, which is $\theta = \theta_I - \pi$.

We next write down the next few key ray optics terms. (To simplify expressions, without losing anything essential, we assume that that the wave is incident on the lower face of the wedge.) The first reflected wave moves in the direction θ_1; has a shadow boundary at the same angle; and has the form

$$\Psi_1^{ray}(r,\theta) = A_1 e^{ikr\cos(\theta-\theta_1)}H(\theta - \theta_1), \ (\phi_1 < \theta < \phi_2). \tag{75}$$

The first transmitted wave within the wedge moves in direction $\theta = \theta_2$ and has the form

$$\Psi_2^{ray}(r,\theta) = A_2 e^{ikrn\cos(\theta-\theta_2)}H(\theta - \theta_2), \ (\phi_2 < \theta < 2\pi + \phi_1) \tag{76}$$

and the wave outside the wedge which is obtained when the above transmitted wave is refracted at the top surface moves in direction $\theta = \theta_3$ and has the form:

$$\Psi_3^{ray}(r,\theta) = A_3 e^{ikr\cos(\theta-\theta_3)}H(\theta - \theta_3), \ (2\pi + \phi_1 < \theta < 2\pi + \phi_2) \tag{77}$$

Attention should be paid to the way we have defined the angles so that the angle θ varies continuously as we pass across boundaries. The fact that Ψ_3 is not defined on the same range as Ψ_1 does not matter of course when the physical field is calculated. The equations defining the angles are obtained straightforwardly and are given by

$$\cos(\phi_2 - \theta_I + \pi) = \cos(\phi_2 - \theta_1) \quad \text{or} \quad \theta_1 = 2\phi_2 - \theta_I - 2\pi, \tag{78}$$

when we pay attention to the correct range of definitions. Also

$$n\cos(\phi_2 - \theta_2) = \cos(\phi_2 - \theta_1) \quad \text{or} \quad \theta_2 = \phi_2 + \cos^{-1}(\cos(\phi_2 - \theta_1)/n), \tag{79}$$

and

$$\cos(\phi_1 - \theta_3) = n\cos(\phi_1 - \theta_2) \text{ or } \theta_3 = 2\pi + \phi_1 + \cos^{-1}(n\cos(\phi_1 - \theta_2)). \tag{80}$$

.

It will be realized that for some values of the physical parameters of the problem this last equation will not yield a real solution. This corresponds to the case of total internal reflection at the upper surface, in which case the second "transmitted" wave will in fact be exponentially decaying: a surface wave. Such waves are of course ignored in a ray optics treatment.

We can also evaluate the coefficients simply. The boundary conditions on the lower face are

$$1 + A_1 = A_2, \quad \sin(\phi_2 - \theta_I + \pi)(1 - A_1) = n\gamma A_2 \sin(\phi_2 - \theta_2) \tag{81}$$

and so

$$A_1 = \frac{\sin(\phi_2 - \theta_I + \pi) - n\gamma \sin(\phi_2 - \theta_2)}{\sin(\phi_2 - \theta_I + \pi) + n\gamma \sin(\phi_2 - \theta_2)} \tag{82}$$

and

$$A_2 = \frac{2\sin(\phi_2 - \theta_I + \pi)}{\sin(\phi_2 - \theta_I + \pi) + n\gamma \sin(\phi_2 - \theta_2)}. \tag{83}$$

For refraction at the upper surface we have similar results, but for our present didactic purposes we only require the transmitted amplitude

$$A_3 = A_2 \frac{2n\gamma \sin(\phi_1 - \theta_2)}{\sin(\phi_1 - \theta_3) + n\gamma \sin(\phi_1 - \theta_2)} \tag{84}$$

It is then clear that any number of reflections and refractions can be handled in the same way. It is only a matter of algebra. There will only be a finite number of ray optics terms, the number depending on the material constants of the wedge and the angle of incidence. In general, of course, the plane waves in the ray optics solution have discontinuities at shadow boundaries. But we have shown, in earlier sections, how such boundaries can be removed to produce fields which ARE solutions of the wave equations. It simply means adding contour integrals over appropriate kernels.

In its general form we can represent the full solution $\Psi(r, \theta)$ as the sum of the ray optics solution and additional terms

$$\Psi(r, \theta) = \Psi^{\text{ray}}(r, \theta) + \Psi^{\text{add}}(r, \theta) \tag{85}$$

where

$$\Psi^{\text{add}}(r,\theta) = \int_D K(z,\theta)e^{ikr\cos z}dz \;\text{ in medium } M_a \tag{86}$$

$$\Psi^{\text{add}}(r,\theta) = \int_\Delta \Xi(\zeta,\theta)e^{ikr\cos\zeta}d\zeta \;\text{ in medium } M_b \tag{87}$$

and D and Δ are contours which have been described in section 3. We next demonstrate how to calculate the kernels $K(z,\theta)$ and $\Xi(z,\theta)$.

8.2 The kernels in the general case

We will find general expressions for the kernels *to all orders of expansion.* We will let M_a be the medium external to the wedge and M_b be internal. A kernel relating to the external medium will be expressed as a sum of partial kernels of the form $K(z \pm \theta)$, in a way made familiar in earlier sections, and a kernel relating to the medium within the wedge will be expressed as a sum of partial kernels of the form $\Xi(\zeta \pm \theta)$. In taking account of the boundary conditions on a surface an incident kernel $K(z \pm \theta)$ gives rise to a reflected kernel $K(z \mp \theta)$ and a refracted kernel $\Xi(\zeta \pm \theta)$. Likewise an incident kernel $\Xi(\zeta \pm \theta)$ gives rise to a reflected kernel $\Xi(\zeta \mp \theta)$ and a refracted kernel $K(z \pm \theta)$.

We will suppose that the incoming plane wave comes from outside the wedge. (It is easy to modify the approach for the other, less common, possibility.) We then, as in all previous problems, add to the ray optics term a line integral with the simple kernel $K_0(z-\theta)$ which models the shadow boundaries of a plane incident wave by adding a cylindrical wave. We then take account of the boundary conditions on the faces of the wedge by adding new terms which correspond to refraction and reflection of the cylindrical wave. These terms are integrals with first order kernels with form $K_1(z+\theta)$ and $\Xi_1(\zeta-\theta)$, (whether they arise from fitting the boundary at the upper boundary, S_1, or the lower one, S_2). We then take these first order terms as incident on the faces and fit the boundary conditions to give second order terms with forms $K_2(z-\theta)$ and $\Xi_2(\zeta+\theta)$ and so on to higher orders. Although it is a little more abstract, we are proceeding very much in the way in which the ray optics solution is obtained, by just calculating iteratively what rays are reflected and refracted at the surfaces. Bearing the above pattern in mind we can then write the *mth* order kernels, which *start* with a reflection at surface S_i as $K_i^m(z-(-1)^m\theta)$ and $\Xi_i^m(\zeta+(-1)^m\theta)$, with $i = 1, 2$.

We now proceed to fill in the algebra of this process. In order to simplify the expressions we will write down separately the expressions for the even orders and odd orders, which means that we avoid a profusion of factors $(-1)^m$. Suppose first that at the mth iteration, with m even, we have fields $K^m(z-\theta)$ and $\Xi^m(\zeta+\theta)$ and then have to find the $m+1$st terms of the iteration by requiring the boundary conditions to be met on $\theta = \phi$. (With these assumptions we will be able to cover all cases by later choosing $\phi = \phi_1, \phi_2$ and also by choosing $\theta = -\theta$.)

Let us call the $m+1$st order term which arises by reflection of $K^m(z-\theta)$, $K_K^{m+1}(z+\theta)$ and that which arises by refraction $\Xi_K^{m+1}(\zeta-\theta)$. Similarly we call the terms arising from $\Xi^m(\zeta+\theta)$, $K_\Xi^{m+1}(z+\theta)$ and $\Xi_\Xi^{m+1}(\zeta-\theta)$. From the work of section 3 and using $K^{m+1} = K_K^{m+1} + K_\Xi^{m+1}$ we then find that

$$K_i^{m+1}(z+\phi_i) = \frac{\zeta'(z)-\gamma}{\zeta'(z)+\gamma} K_i^m(z-\phi_i) + \frac{2\gamma\zeta'(z)}{\gamma+\zeta'(z)} \Xi_i^m(\zeta(z)+\phi_i) \quad (88)$$

$$\Xi_i^{m+1}(\zeta-\phi_i) = \frac{2z'(\zeta)}{1+\gamma z'(\zeta)} K_i^m(z(\zeta)-\phi_i) + \frac{\gamma z'(\zeta)-1}{\gamma z'(\zeta)+1} \Xi_i^m(\zeta+\phi_i). \quad (89)$$

Here $i = 1, 2$ indicates which surface $\phi = \phi_i$ the iteration starts with. Since we are dealing with m even, we are fitting boundary conditions on the same surface that the iteration started with. The corresponding equations for odd values of m are obtained by fitting the boundary condition on surface $\theta = \phi_j$, with $j \neq i$, and also taking account of the change of sign of θ:

$$K_i^{m+1}(z-\phi_j) = \frac{\zeta'(z)-\gamma}{\zeta'(z)+\gamma} K_i^m(z+\phi_j) + \frac{2\gamma\zeta'(z)}{\gamma+\zeta'(z)} \Xi_i^m(\zeta(z)-\phi_j) \quad (90)$$

$$\Xi_i^{m+1}(\zeta+\phi_j) = \frac{2z'(\zeta)}{1+\gamma z'(\zeta)} K_i^m(z(\zeta)+\phi_j) + \frac{\gamma z'(\zeta)-1}{\gamma z'(\zeta)+1} \Xi_i^m(\zeta-\phi_j). \quad (91)$$

The total field is given by adding the kernels corresponding to the series starting with refraction at the bottom ($i = 2$) and top ($i = 1$) surfaces of the wedge. Thus

$$K(z,\theta) = \sum_{m=0}^{\infty} [K_1^m(z-(-1)^m\theta) + K_2^m(z-(-1)^m\theta)] \quad (92)$$

$$\Xi(z,\theta) = \sum_{m=0}^{\infty} [\Xi_1^m(\zeta+(-1)^m\theta) + \Xi_2^m(\zeta+(-1)^m\theta)]. \quad (93)$$

These equations allow all kernels to be calculated iteratively, given only the lowest order terms. If we specialise to the case of an incoming wave from outside the wedge then we have $\Xi^0 = 0$ and the familiar

$$K^0(z) = \frac{-i}{(z+\theta_I)^2 - \pi^2}. \quad (94)$$

The number of terms that will be required is a function of the required accuracy and the physical configuration of interest.

It may be asked if there is any chance of being able analytically to evaluate the sum of the series of kernels, as was possible in some of the simpler problems dealt with earlier in the paper. Our reply is that this is very unlikely. The reasoning is that if the sum has a reasonably simple expression then the result could also be obtained in another way by one of the very fine minds who have worked on this problem previously. Furthermore, since it is not even possible to sum the far simpler ray optics terms, it is improbable in the extreme that the more complex kernels can be summed. However, even if it were possible, it would seem likely that, as in the problems of earlier sections, for practical purposes a few terms only would be needed to give a result more than adequate for most purposes. In short the sum would be of academic rather than practical interest.

With these key results we have provided a tool that can be used in principle to calculate waves scattered by permeable wedges with an enormous range of possible configurations, of interest to different specialists. There are wedges with all different relative physical parameters n and γ. These includes cases in which the wedge may have a lower refractive index than the surrounding medium. There are wedges of all angles from very thin to very obtuse angled. Then there is the exploration of different angles of incidence, not to mention different regions of interest in the scattered field - close or distant to the surface of the wedge, close or distant from the edge. There are far fields or near fields or fields in intermediate regions. In addition those who are interested in electromagnetic scattering have the extra complication of needing to decompose the field into different polarization components. The purpose of this paper is to present as clearly as possible a *method* which of potential value to those interested in any of these areas. It would muddy the water to get too bogged down in details of computation. Consequently we will content ourselves with just taking a step or two down the path to show how things proceed, and leave the exploration of the use of the method in practical applications to later papers by ourselves or others.

Specifically we will look at how the first three ray optics terms mentioned above are modified to be continuous solutions of the wave equation. This demonstration should be enough to show how to obtain any number of terms required for a particular purpose in particular configuration. The kernel corresponding to the field produced by reflection from the lower face ($\theta = \phi_2$) is, from the above results, given by

$$K_2^1(z + \phi_2) = \frac{\zeta'(z) - \gamma}{\zeta'(z) + \gamma} K^0(z - \phi_2). \tag{95}$$

That corresponding to reflection from the upper face ($\theta = \phi_1$) is given by

$$K_1^1(z+\phi_1) = \frac{\zeta'(z)-\gamma}{\zeta'(z)+\gamma} K^0(z-\phi_1). \tag{96}$$

However, in the configuration we have chosen this term has no corresponding ray optics equivalent (though it would have, of course, if the incident field impinged directly on the upper face of the wedge). The contribution can be expected to be comparatively small and for simplicity of presentation and saving of paper we will not include this term here, though anyone concerned with a higher degree of accuracy could do so with little trouble.

The kernel corresponding to the internal wave produced by refraction at the lower surface is given by

$$\Xi_2^1(\zeta-\phi_2) = \frac{2z'(\zeta)}{1+\gamma z'(\zeta)} K^0(z(\zeta)-\phi_2). \tag{97}$$

The kernel corresponding to the wave which arises in the outer region when the internal wave is refracted at the upper surface is given by

$$K_2^2(z+\phi_1) = \frac{2\gamma\zeta'(z)}{\zeta'(z)+\gamma} \Xi_2^1(\zeta(z)+\phi_1). \tag{98}$$

Those are the kernels we will use to exemplify the general patterns that arise. Other terms will follow the same principles, using our general iterative formulae. Thus the next step would be to include the additional, second order, internal wave produced by reflection from the top surface to add to the ray optics reflected wave from that surface. Then there are the various terms of the third and higher order. The kernels can be calculated iteratively, as above. The evaluation techniques are essentially the same as those of the lower order terms we demonstrate.

The question of convergence is one we have not addressed mathematically in this paper. There are good reasons for supposing that there will be little problem in practice. One reason is that in the earlier problems on wedges and wedges where the series solution could be summed explicitly there was no problem. Perhaps a more powerful reason is that the cylindrical scattered waves which smooth out the ray optics solutions must be of the same general order of magnitude as the ray optics terms, and so if we accept that there is no convergence problem with the infinite series of ray optics terms it is hard to see that there can be one with the scattered waves. We conclude that though there is an opportunity for someone to write a paper in which close bounds can be placed on the rates of convergence there is no reason to suppose that for the more practical applications on which this paper is focused there is any need for concern in that area. Indeed in practice we expect that, as in the case of known solutions, it will be found that no more than few terms of the expansion will be needed to give a very adequate accuracy. After all, in many cases all that the experimenter needs is an idea of the order of magnitude of the difference between his readily calculated ray optics solution and the full wave solution, *in shadow regions*. And this is provided by a single integral for each shadow.

With that preamble we can write down the terms of our expansion of the field corresponding to the first three ray optics terms. mentioned above, by adding, as in (85), the ray optics terms calculated in equations (74)- (77) and the integral terms.

$$\Psi_0(r,\theta) = \Psi_0^{ray}(r,\theta) + \int_D K_0(z-\theta)dz \tag{99}$$

$$\Psi_1(r,\theta) = \Psi_1^{ray}(r,\theta) + \int_D K_2^1(z+\theta)dz \tag{100}$$

$$\Psi_2(r,\theta) = \Psi_2^{ray}(r,\theta) + \int_\Delta \Xi_2^1(\zeta-\theta)d\zeta \tag{101}$$

$$\Psi_3(r,\theta) = \Psi_3^{ray}(r,\theta) + \int_D K_2^2(z+\theta)dz, \tag{102}$$

We have already discussed the nature of the contours D and Δ in section 3. They are shown in Figs. 3 and 5 respectively. We now briefly describe some features of the above integrals which depend on the nature of he contours and kernels. The kernel $K_0(z-\theta)$ has two poles and no branch cuts, and so the contour D simplifies to the imaginary axis, as in the easier problems dealt with earlier in the paper. The discontinuity in $\Psi_0^{ray}(r,\theta)$ is, as in earlier cases, exactly balanced by the discontinuity in line integral. The shadow boundary in physical space corresponds to the pole of K_0 lying on D.

The kernel $K_2^1(z-\theta)$ also has two poles, only one of which corresponds to a shadow when the incident wave comes from below the wedge, as we are assuming. The discontinuity at the ray optics shadow boundary is again balanced by the discontinuity in the integral as the corresponding pole crosses the imaginary axis. All that is familiar by now from the work in earlier sections. The novelty that now arises is the existence of the contributions from the branch cuts. These have to do with the existence of boundary waves when there is a discontinuity of refractive index between the media. What happens is that in the region below the lower surface we find the contribution from the cut illustrated in the first part of Fig. 3 yields a field which is exponentially decaying downwards away from the face. In the region outside the wedge and above the (extended) plane of the lower surface we find that the contribution from that cut disappears and that of the other is included, as illustrated in the second part of Fig. 3, and we again have field that decays exponentially away from the wedge. These contributions are therefore only of any interest to experimenters who need the field close to the edge of the wedge. Others may well find that they can neglect them without loss and so ease their calculational burden.

The kernel $\Xi_2^1(\zeta - \theta)$ has two poles and the branch cuts shown in Fig. 5. The poles provide the mechanism to smooth any shadow boundaries, which do not in fact arise in the configuration we are considering, and the branch cuts provide the mechanism to describe the effects of boundary waves. The extra vertical contour is also an effect of a boundary wave, in that it gives a cylindrical wave within the wedge that is needed to balance the boundary wave in the external space, as a result of the mapping between contours D and Δ.

Correspondences like this continue to hold in each term of our general expansion. Each kernel has poles and branch points. The poles are inherited from $K_0(z)$ and deal with the basic transition from a discontinuous ray optics to a continuous wave solution. They are the key feature which enables the shadow boundaries of the ray optics approximation to be smoothed. In many cases this is going to be the dominant correction. The existence of branch points is a feature inherited from the basic nature of refraction, and is the analytic counterpart of the existence of boundary waves. These do add to the burden of accurate computing since they require good detailed accounting to ensure that the complex functions involved are defined on the correctly cut sheets. We believe that the lengthy work in section 3 on the methods of choosing contours will provide all that is needed to deal with these matters.

Conclusion

We have demonstrated a fresh approach to a wide range problems of scattering of waves by edges and wedges, which can replace a variety of different and more difficult approaches. When it is used on problems to which solutions are known, it obtains the solutions in a simpler way. Furthermore the approach yields very useful approximate solutions that give as much accuracy as is normally needed, but for a fraction of the effort. When the approach is applied to the problem of diffraction by a wedge, which has no previously known solution, it gives an explicit analytic solution, which retains the attractive feature that a useful approximate solution can be obtained without having to evaluate ALL the terms in an expansion. We do not seek to conceal the fact that someone who requires to know the field close to the faces of the wedge will face the painstaking task of keeping careful track of key complex functions and branch cuts, which is the analytic counterpart of keeping track of how boundary waves on the two faces of the wedge can bounce from one to the other. However such a person will at least have a tool which CAN be used, where previously there was none.

9 Appendix A. Some series.

Our starting point is the well-known identity (Abramowitz[6])

$$\cot z = \sum_{m=-\infty}^{\infty} \frac{1}{z + m\pi}. \tag{103}$$

This implies that

$$\cot(z - c\pi) - \cot(z + c\pi) = \sum_{m=-\infty}^{\infty} \frac{2\pi c}{(z + m\pi)^2 - c^2\pi^2}. \tag{104}$$

If we now replace z by $z/4$ and replace c by $1/4$ we find

$$4 \sum_{m=-\infty}^{\infty} \frac{2\pi}{(z + 4m\pi)^2 - \pi^2} = \cot(\frac{z-\pi}{4}) - \cot(\frac{z+\pi}{4}) = -2\sec\frac{z}{2}, \tag{105}$$

which is our first required result.

The more general form, useful for the case of wedges, involves alternatively replacing z by $z\pi/2\Psi$ and replacing c by $\pi/2\Psi$. This gives

$$\frac{2\Psi}{\pi} \sum_{m=-\infty}^{\infty} \frac{2\pi}{(z + 2m\Psi)^2 - \pi^2} = \cot\left(\frac{z-\pi}{2\Psi/\pi}\right) - \cot\left(\frac{z+\pi}{2\Psi/\pi}\right), \tag{106}$$

which of course reduces to the above when $\Psi = 2\pi$.

By changing the variable by $\pi/2$ in (104) we find that

$$\tan(z - c\pi) - \tan(z + c\pi) = \sum_{m=-\infty}^{\infty} \frac{-2\pi c}{(z + \frac{2m+1}{2}\pi)^2 - c^2\pi^2}. \tag{107}$$

We can then find a series with alternating signs by adding this to (104). Since $\cot z + \tan z = 2\csc z$ we have

$$\csc(z - c\pi) - \csc(z + c\pi) = \sum_{M=-\infty}^{\infty} \frac{c\pi(-1)^M}{(z + \frac{M}{2}\pi)^2 - c^2\pi^2}. \tag{108}$$

By again making the replacements $z \to z\pi/4\Psi$ and $c \to \pi/4\Psi$ we find

$$\frac{2\Psi}{\pi} \sum_{M=-\infty}^{\infty} \frac{2\pi(-1)^M}{(z+2M\Psi)^2 - \pi^2} = \csc\left(\frac{z-\pi}{2\Psi/\pi}\right) - \csc\left(\frac{z+\pi}{2\Psi/\pi}\right). \tag{109}$$

This is the second required result, which simplifies in the case $\Psi = 2\pi$, where we can use

$$\csc\left(\frac{z-\pi}{4}\right) - \csc\left(\frac{z+\pi}{4}\right) = -2\sqrt{2}\frac{\sin\frac{z}{4}}{\sin\frac{z}{2}} \tag{110}$$

to give

$$\sum_{m=-\infty}^{\infty} \frac{2\pi(-1)^m}{(z+4m\pi)^2 - \pi^2} = -\frac{1}{\sqrt{2}}\frac{\sin\frac{z}{4}}{\sin\frac{z}{2}}. \tag{111}$$

10 Appendix B

In this appendix we simply indicate how the forms of solution that we have obtained in this paper to the problems of scattering of a plane wave by a semi-infinite sheet can be transformed into those obtained by earlier methods by one of us (Rawlins[8]). Rather than overburden this paper with too many details that are unlikely to be of much value we will simply work with one case - the soft-soft case. With this as a guide, the interested reader will then readily be able to perform similar calculations in other cases.

We start with the kernel

$$K_{ss}(z,\theta) = -\frac{1}{2}(\sec\frac{z-\theta+\theta_I}{2} - \sec\frac{z+\theta+\theta_I}{2}). \tag{112}$$

We now change the integration variable from z to $-z$ in the second term and compactly write $w \equiv (z-\theta)/2$ and $v \equiv \theta_I/2$. This gives

$$2K_{ss}(z,\theta) = -\sec(w+v) + \sec(w-v) = \frac{-4\sin w \sin v}{\cos 2w + \cos 2v}, \tag{113}$$

having used the elementary $\cos(w+v) - \cos(w-v) = -2\sin w \sin v$ and $2\cos(w+v)\cos(w-v) = \cos 2w + \cos 2v$.

We now make the crucial change of variable of integration

$$\nu = k\cos 2w = k\cos(z-\theta) \tag{114}$$

and define

$$\kappa = -k\sin 2w = -k\sin(z-\theta)\mathrm{sgn}(y), \tag{115}$$

where $y = r\sin\theta$ in this appendix, so that κ is real and positive when $z = 0$ and then

$$d\nu = \kappa\mathrm{sgn}(y)dz = -2\sin w\cos w dz. \tag{116}$$

We then find that the exponent $kr\cos z = \nu x + \kappa|y|$ and the field becomes

$$\Psi_{ss}(x,y) = \Psi^0_{ss}(x,y) + \sqrt{2k}\sin\frac{\theta_I}{2}\int_C \frac{e^{i(\nu x+\kappa|y|)}}{(\nu + k\cos\theta_I)(k+\nu)^{1/2}}d\nu, \tag{117}$$

where $(k+\nu)^{1/2}$ is $\sqrt{2k}\cos w$, and so is real and positive when $\nu = z = 0$.

The contour C in the above is the contour of stationary phase in the ν-plane, which can be distorted down onto the real axis with the usual convention that the contour will be distorted appropriately about the cuts from $-\infty$ to k and from k to ∞.

The remaining differences between this form and that of Rawlins [8] are a result of different positioning of the sheet, a different magnitude of the incoming wave, and taking account of the fact that θ_I is in this paper the direction *from which* the incoming wave is coming. It is also necessary to take a little care with poles when distorting the contour C, related as they are to shadow boundaries, but this will be no problem to anyone familiar with the usual approach to this type of problem.

A very similar piece of analysis transforms the solution when the surface is hard-hard. The cases hard-soft or soft-hard, which are easily derived by this method was much harder to solve by a different method by one of us earlier [8]. The transformation to show the equivalence of the two methods follows much the same path as above. In all these cases there is no doubt that the present method gives the same accurate result as previous, more complicated, methods.

References

[1] H.M. Macdonald, Electric Waves, C.U.P. (1902).

[2] M.J. Kontorowich and N.N. Lebedev, *J. Phys. U.S.S.R* **1**, (1939), p. 229.

[3] N. Wiener and E. Hopf, *S.B. Preuss. Akad. Wiss.*, (1931).

[4] A.D. Rawlins, The solution of a mixed boundary value problem in the theory of diffraction, *J. Engineering Maths* **18**, (1984), pp. 37–62.

[5] A.D. Rawlins, Diffraction by, or diffusion into, a penetrable wedge, *Proc. Roy. Soc. Lond. A* **455**, (1999), pp. 2655–2686.

[6] M. Abramowitz and Irene A. Segun, Handbook of Mathematical Tables, Dover, (1965).

[7] D. S. Jones, The Theory of Electromagnetism, Pergamon, (1964).

[8] A.D. Rawlins, The solution of a mixed boundary value problem in the theory of diffraction by a semi-infinite plane, *Proc. Roy. Soc. Lond. A.* **346**, (1975), pp. 469-484.

[9] A. Somerfeld, *Math. Anal.* **47**, (1896).

[10] B. Budaev, Diffraction by wedges, Longman Scientific & Technical, (1995).

[11] G.D. Maliuzhinets, Excitation, reflection and emission of surface waves from a wedge with given face impedances, *Sov. Phys. Dokl.* **3**, (1958), pp. 752–5.

[12] A.D. Rawlins, A Greens function for diffraction by a rational wedge, *Math. Proc. Camb. Phil. Soc.* **102**, (1989).